Macromolecular Materials and Engineering

Macromolecular Materials and Engineering Open Access
www.mame-journal.de

RESEARCH ARTICLE OPEN ACCESS

PEG-Dialdehydes/Hyperbranched Amines Based Hydrogels and their Potential as Futures Bone Adhesives

Kyriakos Karakyriazis[1,2] | Sebastian Stößlein[3] | Andreas Hartwig[1,2,4]

[1]Fraunhofer Institute For Manufacturing Technology and Advanced Materials, Bremen, Germany | [2]Department 2 Biology/Chemistry, University of Bremen, Bremen, Germany | [3]Purenum GmbH, Bremen, Germany | [4]MAPEX Center for Materials and Processes, University of Bremen, Bremen, Germany

Correspondence: Andreas Hartwig (andreas.hartwig@ifam.fraunhofer.de)

Received: 5 May 2025 | **Revised:** 5 September 2025 | **Accepted:** 16 September 2025

Funding: German Ministry for Education and Research (BMBF), program GO-Bio (project mediGLUE), grant number 161B0393.

Keywords: biomedical adhesives | bone adhesives | hydrogels | imine crosslinks

ABSTRACT

The potential of aminoterminated hyperbranched polyglycerol (hPG-NH_2) crosslinked by polyethylene glycol dialdehyde (DA) hydrogel as a bone adhesive is presented in this proof-of-concept study. The hydrogel system, crosslinked by Schiff base bonds, is designed to degrade hydrolytically when applied internally. To elaborate the relationship between the crosslinker length and the material properties, three different DAs with different molecular masses were used, as well as glutaraldehyde, and also blends of those components. It was shown that the hydrogel's properties could be adjusted by application of these aldehydes and their mixtures. In general, the gelation time decreases with lower molecular mass of the dialdehyde crosslinker, whereas the gel strength increases. The hydrogel model adhesives lead to a bond strength of up to 800 kPA on bone substrates.

1 | Introduction

Bone fractures are one of the most common reasons for hospitalization [1]. Besides the simpler and smoother bone fractures, there are more complex ones like comminuted fractures, that require a surgical procedure and internal fixation of the bone fragments [1, 2]. Commonly used osteosynthesis materials include wires, nails, screws, and plates, which need to be removed by a second operation, leading to higher health risks for the patient and higher costs for the health sector [1]. In the search for an alternative, the focus lies on developing bone adhesives for these situations. Due to the very specific requirements regarding the mechanical strength, cytocompatibility, bioresorbability, and commercialization, no adhesive has been developed that matches all the requirements [1, 3, 4]. Different approaches have been made, including biomimetic-inspired adhesives based on 3,4-dihydroxyphenylalanine (DOPA), biobased adhesives based on sugars and proteins (fibrin, chitosan, etc.) showing low adhesion strength, and methacrylates/ cyanoacrylates coming with poor cytocompatibility and degradation. In a recent study, Shem Tov et al. reported a biodegradable hotmelt adhesive based on poly(ε-caprolactone) blended with 3,4-dihydroxyhydrocinnamic acid and monobasic calcium phosphate [5].

Hydrolytical degradability, due to the reversible nature of the bond, is one of the main reasons why Schiff base chemistry has drawn a lot of interest in the biomedical field in recent years [6]. The main side product of the Schiff base formation, being water, which does not pose any health risks, makes them ideal candidates for biomedical applications. The fast reaction rate, the nontoxic byproducts, as well as the reversibility of the reaction make Schiff base crosslinks very promising candidates for biomedical applications [6]. Schiff base crosslinked hydrogels have been recently utilized for several biomedical applications like tissue engineering [7, 8], drug delivery [9–11], and wound healing [12, 13]. Despite their utilization in hydrogel formulations,

there have been reports of Schiff-base crosslinks also in the field of biomedical adhesives. BioGlue is a sealant used for cardiac surgery, produced by Cryolife Inc. (Atlanta, USA), which consists of glutaraldehyde (GA) and bovine serum albumin (BSA), and has been approved by the FDA [14]. However, the use of the toxic GA and the release of it has raised concerns about the application of this sealant, as reported by Fürst et al. [15]. In 2009, Artzi reported the synthesis of a sealant adhesive formed by the reaction between dextran aldehyde and PEG amine, showing promising results for soft tissues [16]. Ren et al. introduced a hybrid adhesive that utilizes the primary amines of a branched polyamine for a Schiff-reaction with the aldehydes, as well as Michael addition with the double bonds of p-formylphenyl acrylate [17]. The dextran aldehyde was also used by Hegazy and Moon et al. to cross-link a polyaspartamide-aldehyde to form an adhesive, showing low cytotoxicity, self-healing properties, and high adhesion strength on soft tissues [18]. Another hybrid adhesive system was reported by Yang et al., which consists of the copolymer of 3-Aminopropyl methacrylamide and Trishydroxymethyl methacrylamide crosslinked with oxidized methylcellulose. The reported adhesive crosslinks both covalently via Schiff-base linkages and high-density hydrogen bonds and is proposed to be used for bone retention in maxillofacial surgery [19]. Nishiguchi et al. reported a tissue adhesive based on Alaskan pollock gelatin as a hemostatic agent [20]. The gelatin was modified with decyl groups via Schiff base formation, followed by a reductive amination [20, 21].

Hyperbranched polyglycerols (hPG) have attracted much attention in recent years as an alternative for polyethylene glycol (PEG) dendrimers, due to their topology and facile synthesis [22, 23]. Their polyether backbone provides them with excellent cytocompatibility and hydrophilicity, while their multiple end-standing groups pose ideal sites for functionalization [22]. hPG also shows a major advantage compared to other hydrogels, which is the low viscosity of precursor solutions, which can be utilized to form gels with very high solid contents, yielding stronger hydrogels [24]. Recent advances in the field of hPG-hydrogels propose diverse cross-linked systems for many biomedical applications, like tissue engineering and drug delivery. Oudshoorn et al. introduced a simple synthesis of hPG-methacrylate and its gels after polymerization of the methacrylate groups via a variety of crosslinkers and catalysts, which show promising results in tissue engineering and drug delivery systems [24]. Steinhilber et al. introduced disulfide crosslinks as biodegradation sites in their hydrogels, as degradable scaffolds to transport and deliver bioactive substances [25, 26]. Another strategy to actively introduce degradation sites to the hydrogels has been recently reported by Dos Campos et al. by crosslinking hPG with oxalic acid via pH-sensitive, hydrolytically degradable ester bonds, to release drugs in a controlled way [27]. Further crosslinking approaches include crosslinking with di- or triepoxides, different double-bond baring moieties, and azide-cyclooctyne reactions, with an intended use as drug carriers or in tissue engineering [28–33].

In this manuscript, a previously published hyperbranched aminoterminated polyglycerol/polyethylene glycol dialdehyde (hPG-NH_2/ DA) hydrogel [34] is tested on its potential use as a bone adhesive. The target application is the fixation of small bone fragments during surgery. The required degradability is achieved by introducing Schiff-base bonds as crosslinks in the polymer backbone that can later hydrolytically degrade while the bone heals. The focus of this work is on the effect of dialdehyde (DA) crosslinkers with different molecular weight and their effect on the mechanical properties of the resulting adhesive hydrogel. The amino terminated hPG (hPG-NH_2) part is not changed for these examinations. It is proposed that by using the selected dialdehydes and their mixtures, gel strength, gelation time, and adhesion properties on polymer and bone substrates can be adjusted.

2 | Experimental Section

2.1 | Materials

All chemicals were purchased from Sigma–Aldrich (Steinheim, Germany) and used as received. Exceptions were documented.

2.2 | NMR-Characterization

^{1}H-NMR spectra were recorded on a AVANCE NEO 600MHz-spectrometer (Bruker, Ettlingen, Germany). The sample concentration was chosen at 10 mg/mL either in D_2O or DMSO-d6, purchased by Deutero GmbH, Kastellaun, Germany. The spectra were processed with MestReNova 10.0.2-15465 (Mestrelab Research, Santiago de Compostela, Spain).

2.3 | Synthesis of Aminoterminated Hyperbranched Polyglycerol hPG-NH_2

Aminoterminated hyperbranched polyglycerol hPG-NH2 was prepared in a two-step synthetic procedure as described in detail previously (Scheme 1) [34]. In the first step, hPG-co-AGE was synthesized as established by Sunder et al. [35], by anionic ring-opening polymerization of glycidol using 1,1,1-tris(hydroxymethyl)-propane (TMP) (0.536 g, 3.996 mmol, 1 eq.) as initiator, which was partially deprotonated by potassium methanolate (83.04 mg, 0.3 eq). 12.32 g glycidol (41.6 eq.) and 11.55 g allylglycidylether (25.3 eq.) were added dropwise and polymerized at 90°C via anionic ring-opening polymerization. In the second step, hPG-co-AGE (8 g) underwent a photoinitiated thiolene coupling reaction in 90 mL methanol with 3.3 g cysteamine and 0.1 g Irgacure 2959 as photoinitiator. The crude product mixture was dialyzed against ddH_2O with a molecular weight cut-off of 1 kDa and lyophilized, to yield the desired hPG-NH_2.

^{1}H-NMR (D_2O) δ 0,76-0,82 (s, 3H, H-1); 1,23-1,29 (m, 2H, H-2); 1,78-1,88 (s, 2H, H-11); 2,54-2,63 (m, 4H, H-12, H-13); 2,71-2,79 (m, 2H, H-14), 3,27-3,97 (m, ≈ 250H H-3-6, H-10); 3,99-4,07 (s, 2H, H-7); 5,19-5,34 (dd, 2H, H-8); 5,85-5,95 (m, 1H, H-9)

2.4 | One-Pot Synthesis of the Dialdehydes DA-X

DA-X was synthesized and purified by the previously reported procedure [34]. In short: Three different PEGs were dried and used as starting molecules (Table 1) and were functionalized first with isophorone diisocyanate (IPDI) in the presence of Borchi

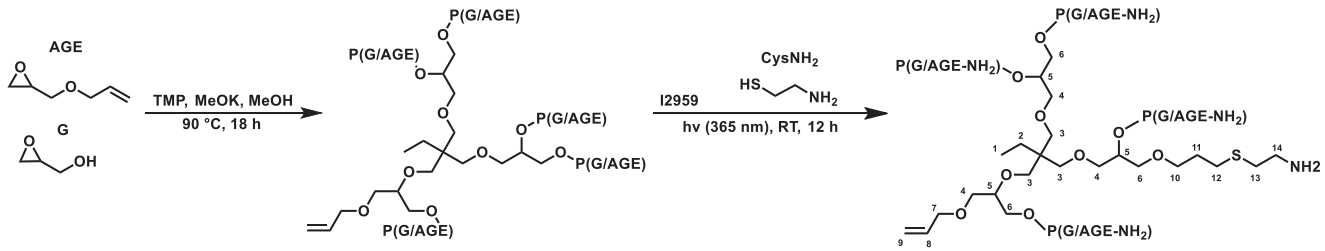

SCHEME 1 | Synthesis of hPG-NH_2.

TABLE 1 | Composition of reaction mixtures and educt amounts used for the synthesis of the DA-X.

Name	Mw(PEG) (g mol^{-1})	m(PEG) (g)	m(Borchi Kat.0244) [mg]	m(IPDI) (g)	m(HMF) (g)	HMF-content (w%)
DA-1	1000	60.4	20.4	46.0	26.8	8.98
DA-2	1500	25.8	10.0	8.1	4.9	6.99
DA-3	3000	59.1	19.8	8.9	5.2	4.06

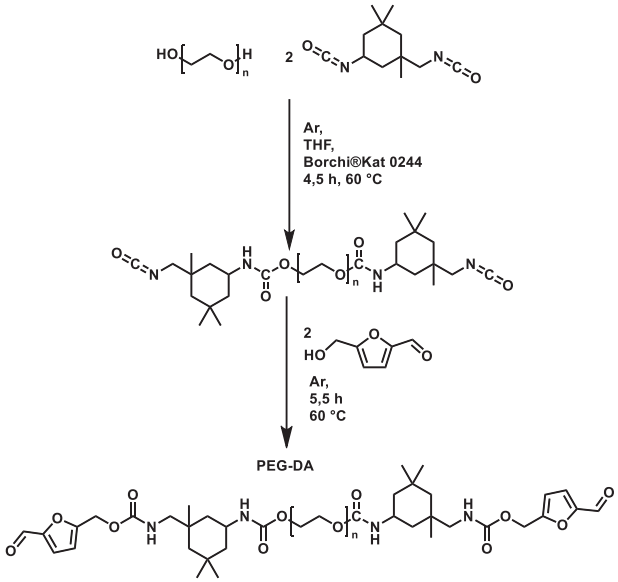

SCHEME 2 | Synthetic route of DA-X.

Kat 0244 (Bi and Zn-based catalyst from Borchers, Langenfeld, Germany) and later with hydroxymethylfurfural (HMF) to yield the respective DA-X as shown in Scheme 2. The crude product was dissolved in methanol and precipitated.

2.5 | Determination of the Aldehyde (CHO)-Content and the Average Molecular Weight of the DA

The CHO-content of the DA-X was determined as reported [34] by using a SPECORD210 PLUS Spektralphotometer (Analytik Jena GmbH, Jena, Germany) in a range from 190–400 nm. The recording and evaluation of the spectra was carried out using the software WinASPECT PLUS (version 4.2.0.0). The average molecular weight was calculated from the HMF-content (Table 1), assuming that every DA-X molecule possesses two aldehyde groups.

2.6 | Hydrogel Formation

To prepare the hydrogels, two water-based prepolymer solutions, one of hPG-NH_2 and one containing dialdehydes, were mixed. The molar concentrations of these polymers in the gel were adjusted as needed to maintain a constant solid content of 12.5 w% and an equimolar ratio of aldehyde to amine groups. The solid content was chosen at 12.5 w% based on our previous work and on the limitations of the characterization methods described in the following [34]. This was to ensure that all materials could be measured with the same equipment and setup. The two solutions were placed in 5 mL two-component syringes (ACHEM GmbH, Germany) equipped with a static mixer. The reaction mixture was then poured into a well of a 24-well plate and sealed to allow for complete curing over a period of 22 h. As the curing time varies from formulation to formulation 22 h were chosen to ensure completeness.

2.7 | Measurement of the Hydrogel Strength

The strength of the gel was assessed using a TA.XTplusC Texture Analyser (Stable Micro Systems, Godalming, UK). The device was equipped with a 5 kg loadcell and a P/0.5 plunge. After curing over a period of 22 h, the gels were directly measured in the well-plate. The plunger was set to descend with a speed of 0.5 mm/s. The data recording started after contacting the gel surface and detecting a resisting force of 4.2 mN. After this point, the plunger continues descending further 4 mm, compressing the hydrogel and recording the opposing force. The highest load recorded during this process was defined as the gel strength (Supporting Information Figures S1-S13).

2.8 | Measurement of the Gelation Time

The definition of gelation time refers to the duration within which a material remains workable and can be processed before the viscosity becomes too high. The gelation time is an important aspect for future applications in surgical procedures. Optimal

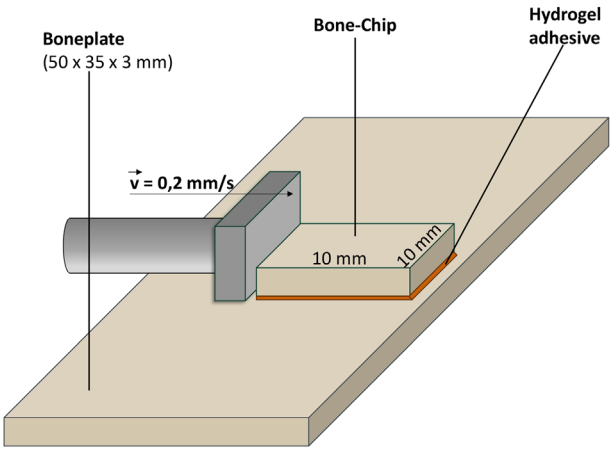

FIGURE 1 | Experimental setup for the adhesion tests of bone substrates with the bond tester.

gelation times depend on the complexity of the bone fracture would be from 15 to 100 s. Within this time frame, the materials can be applied and cure quickly enough to avoid waiting times during surgery. To measure the gelation time of the adhesive hydrogels the TA.XTplusC texture analyzer was used with a 5 kg loadcell and a P/0.5 plunge. In this experiment, the plunger was placed at an initial height of 13 mm above the well plate. Starting with the hydrogel formation by injecting the reaction mixture, the plunger started descending for 17 mm with a speed of 6 mm/s until it immersed 3 mm deep into the sol. After the penetration of the mixture, the plunger is drawn back at the same speed until the cycle starts again at 13 mm over the well plate. These 5.66 s cycles were continued, and the number of cycles until a thread of hydrogel persisted between the plunger at the starting position and the well plate was noted.

2.9 | Measurement of the Adhesive Strength

The adhesion properties were tested on substrates consisting of PA6 filled with 40 w% hydroxyapatite as an artificial bone model prepared by Rocholl GmbH (Eschelbronn, Germany). A part of the specimens received (120 × 10 × 3 mm) were cut into smaller plates of 10 × 10 × 3 mm. In this way, several smaller platelets could be tested on one bigger substrate. The hydrogel reaction mixture was applied with a two-component syringe on the larger substrate. Following the hydrogel application, the smaller plates were immediately positioned on top of the reaction mixture and left to cure for 12 h. During this time, the specimens were covered with a plastic cover to avoid uncontrolled drying. The adhesive bonds were tested with a bond tester (Nordson DAGE 4000PLUS, Westlake, Ohio, USA) at a speed of 2 mm/s, equipped with a 20 kg load cell.

Complementary to the PA6 substrates, bovine bone substrates were also used to investigate the adhesion of the hydrogels. The bones were prepared as previously reported by Lührs et al. and were then cut into smaller 10 × 10 × 3 mm platelets. The measurement setup was the same as for the PA6 specimens [36] (Figure 1).

3 | Results and Discussion

3.1 | Synthesis of the Dialdehydes DA-X

Three different DA-X with increasing molecular weight were synthesized as described in Table 2. The lowest molecular weight candidate DA-1 was synthesized with PEG of 1 kDa, resulting in a DA with an average molecular weight of 2806 g mol^{-1}. The large nonpolar IPDI-groups lowered the polarity of the product to a degree that it was not water-soluble anymore and could not be used further for the formation of hydrogels. In a second approach, PEG of 1.5 kDa was implemented in the described synthetic procedure, resulting in DA-2 with an average molecular weight of 3607 g mol^{-1}. The third DA (DA-3)—created with a PEG of 3 kDa, was the already established DA from our previous publication [34] with an average molecular weight of 6218 g mol^{-1}.

3.2 | Characterization of the Hydrogels with the Different DAs: Gelation Time and Gel Strength

The dialdehydes were dissolved in water and mixed with aqueous solutions of hPG-NH_2 to form hydrogels at an equimolar amine to aldehyde ratio and a total solid content of 12.5 w% in every setup. To push the limits, glutaraldehyde was used as the lowest molecular weight dialdehyde with a molar mass of 100 g mol^{-1}. The formulation with glutaraldehyde precipitated in just a few seconds, resulting in a very brittle material, lacking hydrogel and adhesive properties. As DA-1 was not soluble in water, it could not be implemented for the formulation of hydrogels. The use of a co-solvent to enable the formation of hydrogels with DA-1 was not further pursued, as the adhesive system would not be purely water-based, so that a systematic comparison with the other hydrogels would not be possible. A structural modification of DA-1 would also lead to altered results and would not solely show the effect of the DA length on the hydrogel properties. The gels with DA-2 showed a lower gelation time than those with DA-3 as shown in Table 2, which can be attributed to the different spacer lengths. As DA-2 is much smaller than DA-3, it can move easier within the reaction mixture and reach the reactive sites faster. The gel strength, on the contrary, showed only a slight increase, due to the higher cross-link density induced by the smaller DA-2. As a reference to the different formulations, a BSA-GA adhesive inspired by the commercially available soft tissue adhesive BioGlue was chosen. While BioGlue originally has a solid content of about 30 w%, for this experiment, the solid content was decreased to 12.5 w% to match the solid contents of the hPG/DA-X formulations. The BSA/GA showed a significantly higher gelation time of around 6 min. The gel strength of the BSA-GA, on the other hand, with 15.5 N, was lower than that measured for both the DA-X gels.

3.3 | Blending the Aldehyde Components

To further investigate the impact of the composition on the gelation time and the gel strength of the system, the DA-2 and DA-3 were blended at different mass ratios. The gel's overall solid content (w%) remained constant. To effectively examine the impact of the blends, the aldehyde component mass ratios were altered according to the following equation. $w\%\ (CHO1) =$

TABLE 2 | Overview of the different formulations regarding their gelation time and their gel strength.

Formulation	Mw of aldehyde (g mol^{-1})	Average PEG-units	Gelation time (s)	Gel strength (N)
hPG/GA	100	0	—	—
hPG/DA-1	2806	22	—	—
hPG/DA-2	3607	34	102	20.9 ± 1.9
hPG/DA-3	6218	68	166	17.7 ± 1.9
BSA/GA	100	0	480	15.5 ± 1.3

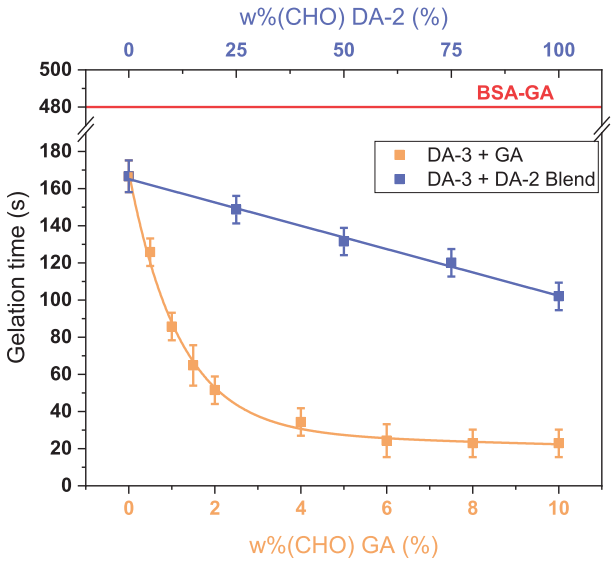

FIGURE 2 | Gelation time in dependence of the GA (yellow) and the DA-2 (blue) w%(CHO) in a blend with the dialdehyde DA-3 in comparison to the BSA-GA adhesive.

$\frac{m(CHO1)}{m(CHO1)+m(CHO2)} \times 100\%$ where CHO1 is the first dialdehyde and CHO2 the second dialdehyde of the blend. At the same time, DA-3 was also blended with glutaraldehyde to observe the effect of the smallest possible dialdehyde on the gel properties. As glutaraldehyde solely did not yield any gels, it was blended in small amounts with the larger dialdehydes (w%(CHO) ≤ 10) than the DAs (0< w%(CHO) < 100), to form hydrogels.

3.4 | Effect of Blending on the Gelation Time

Starting with the pure DA-3 formulation, blending with the shorter DA-2 showed a linear decrease in the gelation time, as expected from the results of the pure DAs. (Figure 2) This feature would allow for precise adjustment of the gelation time, depending on the required applications.

The addition of glutaraldehyde to the original formulation of hPG/DA-3 lead to a rapid decrease in the gelation time. Even at very low w%(CHO) of 1%, the gelation time already dropped to 65 s. The decline of the gelation time continued up to 24 s (± 5.6 s = cycle time) at 6 w% glutaraldehyde. This shows that in future product development glutaraldehyde could be used as an accelerator, to achieve even lower gelation time values, if desired.

Compared to the linear decrease in the gelation time for the blend consisting of DA-2 and DA-3, the formulations containing glutaraldehyde showed an exponential decay with increasing glutaraldehyde content. This can be attributed to the much lower size of glutaraldehyde. As the reaction kinetics of the hydrogel formation depend on the diffusivity of the molecules in the polymer mixture, the reaction rate of glutaraldehyde is much higher than the one of any DA-X. By the addition of glutaraldehyde, the gelation becomes much faster, and the imine formation of glutaraldehyde with hPG-NH_2 is sufficient to increase the viscosity. Compared to the gelation time decrease with DA-2, glutaraldehyde accelerates the process much strongly, making it a suitable accelerator for future formulations.

3.5 | Effect of Blending on the Hydrogel Mechanical Strength

Regarding the mechanical strength of the hydrogels, the bulk formulations with DA-2 and DA-3 showed similar values (20.9±1.9 N for hPG-NH_2/DA-2 and 17.7 ± 1.9 N for hPG-NH_2/DA-3). As expected, the blends of DA-2 and DA-3 presented values in the range of the two unblended DA-X. A slight trend can be interpreted, but cannot be clearly claimed, due to the relatively high standard deviations. This shows that the curing time can be manipulated as desired (Figure 2) without significantly affecting the mechanical properties of the hydrogel (Figure 3).

On the other hand, the addition of glutaraldehyde to the DA-3 affected the mechanical properties of the gels drastically. A very sharp increase in gel strength could be observed at low glutaraldehyde concentrations, reaching a maximum of 45 N at 2 w%(CHO). Interestingly, with a further increase in the glutaraldehyde content, the gel strength decreased. These phenomena can be ascribed to a rising brittleness of the hydrogels that was observed in general by the addition of glutaraldehyde. The negative impact on the hydrogel strength was observed at concentrations of 4 w%(CHO) and above. Compared to the other DA-X blends (DA-2/DA-3), the addition of glutaraldehyde showed a much bigger impact on the hydrogels. Both the rapid increase in the gel strength, as well as the brittleness, can be explained by the increasing cross-link density. While in the other DA blend, the cross-link density just gets slightly higher, the addition of glutaraldehyde drastically increases the cross-link density, leading to the observed effects. The effect of the glutaraldehyde opens the possibility that low concentrations of it (w%(CHO) < 4%) can be implemented as a hardener for the hydrogels. However, it also drastically decreases the gelation time, which needs to be considered if used.

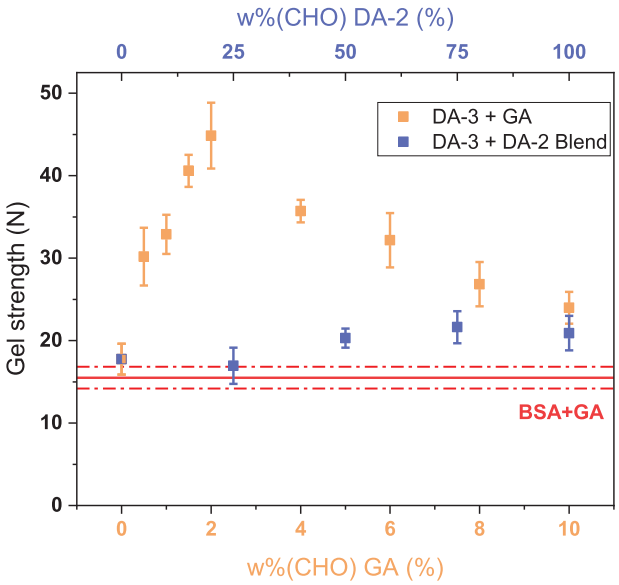

FIGURE 3 | Gel strength in dependence of the GA (yellow) and the DA-2 (blue) w%(CHO) in the dialdehyde component based on DA-3 in comparison to the BSA-GA adhesive.

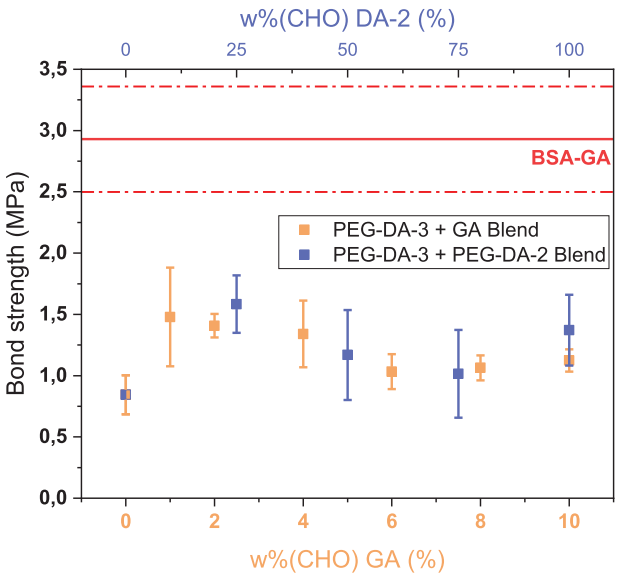

FIGURE 4 | Bond strength in dependence of the GA (yellow) and the DA-2 (blue) w%(CHO) in the dialdehyde component, measured on PA6 substrates in comparison to the BSA-GA adhesive.

3.6 | Adhesion Properties

Additionally, to the described properties, the adhesion properties of the hydrogels were studied. First, they were examined on PA6 substrates filled with 40 w% hydroxyapatite to resemble the bone composition. This substrate serves as a model mimicking bone as it is more readily available, long-term stable, and more reproducible than natural bone. To have reproducible results, all the adhesive hydrogel formulations were cured for 12 h. In this process, the hydrogels between the two substrates were partially dried and formed an adhesive film. The bond strength increases both with increasing DA-2 content as well as with increasing glutaraldehyde content. Like the gel strength, the blending of DA-2 and DA-3 did not show any clear trend regarding the bond strength.

The adhesion strength rose at low w%(CHO), while at w%(CHO) > 4% the strength dropped to lower levels. The BSA/GA adhesive showed a higher adhesion strength than all examined hPG/DA formulations. Overall, the measured bond strengths show no clear correlation to the mechanical strength of the hydrogel adhesive. The BSA/GA reference presenting the lowest gel strength (Figure 3) has the highest bond strength (Figure 4). Concurrently, the hPG/DA-3+GA formulations do not show any difference to the hPG/DA-3+DA-2 blends in the adhesion strength, while the respective gel stabilities reach much higher values.

In a second approach the adhesive strength of the hPG/DA-3 hydrogels with different glutaraldehyde content w%(CHO), was examined on bone substrates. Compared to the polymer substrates, the bond strength decreased to below 1 MPa. In general, a high standard deviation is observed, which can be attributed to the small chip surfaces, as well as the low shear strength of the cured and dried hydrogel adhesive, and also the inhomogeneity of the natural bone substrate. The standard deviations were relatively high, although considering the biological origin of the substrates, in a reasonable range of < 20% [36]. Surprisingly, opposed to the results in the gel strength and the examinations with the PA6 substrates, the adhesion strength was not significantly affected by the addition of glutaraldehyde. The overall decrease in the adhesion strength of both the reference and the hPG/DA-3/GA formulation can be attributed to the substrate's surface. While the bones exhibit a porous surface, the PA6 substrate exhibits a rough surface, which was just sanded. In combination with the low starting viscosity of the applied reaction mixture, it partially penetrates the pores, resulting in a thin adhesive layer. This material loss explains the lower adhesion strength on the bone substrates. In addition to the substrate structure, the substrate material also plays an important role in interfacial interactions. The bone substrates consist mostly of minerals and especially hydroxyapatite, bound in a collagen matrix. The PA6 substrates, on the other hand, are a predominantly organic material, allowing for more molecular interactions such as VdW-interactions, H-Bonds, and coordinative bonds. The synergistic effect of those accumulated molecular interactions would also explain why the adhesive hydrogel is performing better on the PA-6 substrate than on the bone substrate [37].

Further research should take this into consideration and implement a thickener in the hydrogel formulations. We intended to carry out all experiments with the same compositions to figure out the relations between the different properties of the formulations. An additional approach would be to consider priming the bone fragments. This would however, require further research regarding a cytocompatible primer suitable for the proposed adhesive system.

In the adhesion tests, the BSA/GA adhesive outperformed the hPG/DA-X hydrogels on the PA6 substrates with 2.8 MPa compared to values around 1.5 MPa. On the bone substrates, however, the BSA/GA reference showed similar results as hPG/DA-3+GA hydrogels below 1 MPa, showing that the hPG/DA-3+GA for-

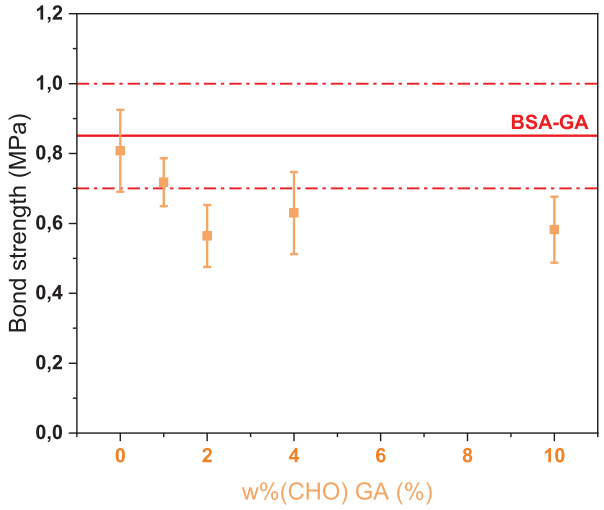

FIGURE 5 | Bond strength of hPG/DA-3 adhesives on bone in dependence on the GA-content in the dialdehyde component based on DA-3 in comparison to the BSA-GA adhesive.

mulations result in similar values in bone adhesion, despite the differences in gel strength and in bond strength on PA6 (Figure 5).

4 | Conclusions

The hydrogel system consisting of hPG-NH_2 and dialdehydes was investigated regarding the influence of the dialdehyde crosslinker length on its properties. Glutaraldehyde was chosen as the shortest dialdehyde crosslinker, while three different DA-X were synthesized to expand the spectrum of crosslinkers. Starting from glutaraldehyde as the DA with the lowest molecular weight, no gel could be formed, as the high cross-link density led to a hard and brittle material with neither adhesive nor hydrogel properties. DA-1 (2.8 kDa) could not be implemented in the hydrogel formation, as it is not soluble in water, due to the large nonpolar content based on IPDI moieties. DA-2 (3.6 kDa) showed formation of a hydrogel, same as DA-3 (6.2 kDa), leading to a longer gelation time than DA-2. This is caused by the shorter spacer length of DA-2, allowing the molecules to diffuse faster to the reaction sites as well as leading to a higher cross-link density.

To investigate and understand the dynamics of shorter crosslinkers on the system's properties DA-3 was blended with DA-2 and with the much shorter glutaraldehyde. While blending DA-3 and DA-2 the gelation time showed a linear relation, decreasing with higher w%(CHO) of the shorter DA-2. The gel strength of the hydrogel adhesive was not significantly affected by blending the two dialdehydes. This shows that blending of DA-2 and DA-3 enables the adjustment of the gelation time with only a minor impact on the gel strength.

The addition of glutaraldehyde led to a much higher reaction rate and a very fast gelation down to 24 s. Contrary to an expected linear relation as shown for the blends with DA-2, glutaraldehyde manifested a rapid decrease in the gelation time until reaching a plateau at 6 w%(CHO), after which no further decrease could be observed. Even at very low w%(CHO) glutaraldehyde had a drastic impact on the gelation time, confirming the importance of the crosslinker's mobility in the reaction mixture. The gel strength, on the other hand, showed a sharp increase, reaching a maximum of 45 N at 2 w%(CHO), before decreasing again. The addition of higher glutaraldehyde quantities leads to a much higher cross-link density, causing brittleness in the resulting hydrogel. The brittleness caused by higher GA concentrations may pose complications in clinical applications. Nonetheless, it was shown that already very low glutaraldehyde amounts reduced the gelation time while increasing the gel strength. Thus, glutaraldehyde could be considered as an additive at w%(CHO) below 2%. This is the case if only the mechanical properties are considered and not toxicity, which was not the subject of our examinations.

The adhesion tests on PA6 substrates filled with 40 w% hydroxyapatite did not show any significant differences between the different hPG/DA-X blends, not even after the addition of glutaraldehyde, which manifests that the gel strength does not directly correlate with the bond strength. The hPG/DA-3+GA formulations were furtherly examined on bovine bone specimens, on which the adhesion strength decreased with the addition of glutaraldehyde, confirming that the gel strength cannot be used as an indication for the resulting bond strength of the applied formulation.

Overall, we were able to show the importance of the crosslinkers' length on the mechanical properties of the hydrogels. The gelation times of hPG-NH_2 adhesives ranged from 3 min to twenty seconds, presenting optimal handling times for future clinical implementations. The adjustability of the gelation time by modifying the length of the DA while being able to keep similar mechanical properties is an additional advantage. The addition of glutaraldehyde resulted in the acceleration of hardening, which could be useful in future applications, while minimizing the amount used due to its toxicity. Future research should test further alternatives of dialdehydes, such as oxidized polysaccharides like dextran [38], alginate, and hyaluronic acid [39], to take glutaraldehyde completely out of the formulation. On bone substrates, the addition of glutaraldehyde as a hardener did not show any effect. In conclusion, the presented system has the potential to be further developed into an applicable bone adhesive. For this experimental confirmation of the expected good cytocompatibility must be the first step, as this was not the content of the presented study.

Author Contributions

Kyriakos Karakyriazis: conceptualization, investigation, visualization, writing – original draft. **Sebastian Stößlein:** supervision, writing – review and editing, **Andreas Hartwig:** supervision, writing – review and editing, basic concept of the system.

Acknowledgements

This work was supported by the German Ministry for Education and Research (BMBF) in the program GO-Bio (project mediGLUE), grant number 161B0393. The support is gratefully acknowledged.

Open access funding enabled and organized by Projekt DEAL.

Conflicts of Interest

The authors declare no conflicts of interest.

Data Availability Statement

The data that support the findings of this study are available from the corresponding author upon reasonable request.

References

1. K. O. Böker, K. Richter, K. Jäckle, et al., "Current State of Bone Adhesives-Necessities and Hurdles," *Materials* 12 (2019): 3975.

2. P. Augat and C. Von Rüden, "Evolution of Fracture Treatment with Bone Plates," *Injury* 49 (2018): S2–S7.

3. M. J. Sánchez-Fernández, H. Hammoudeh, R. P. Félix Lanao, M. Van Erk, J. C. M. Van Hest, and S. C. G. Leeuwenburgh, "Bone-Adhesive Materials: Clinical Requirements, Mechanisms of Action, and Future Perspective," *Advanced Materials Interfaces* 6, no. 4 (2019): 1802021.

4. D. F. Farrar, "Bone Adhesives for Trauma Surgery: A Review of Challenges and Developments," *International Journal of Adhesion and Adhesives* 33 (2012): 89–97.

5. O. S. Tov, A. L. Dotan, and D. Y. Lewitus, "Rational Design of Hot-Melt Biodegradable Tissue Adhesive for Bone Fracture Repair," *Polymers for Advanced Techs* 35 (2024): 70022.

6. J. Xu, Y. Liu, and S. H. Hsu, "Hydrogels Based on Schiff Base Linkages for Biomedical Applications," *Molecules* 24, no. 16 (2019): 3005.

7. T. C. Tseng, L. Tao, F. Y. Hsieh, Y. Wei, I. M. Chiu, and S.-H. Hsu, "Self-Healing Hydrogel to Repair the Central Nervous System," *Advanced Materials* 27 (2015): 3518–3524.

8. F. Y. Hsieh, L. Tao, Y. Wei, and S. H. Hsu, "A novel biodegradable self-healing hydrogel to induce blood capillary formation," *NPG Asia Materials* 9, no. 3 (2017): e363–e363.

9. J. Huang, Y. Deng, J. Ren, et al., "Novel In Situ Forming Hydrogel Based on Xanthan and Chitosan Re-Gelifying in Liquids for Local Drug Delivery," *Carbohydrate Polymers* 186 (2018): 54–63.

10. X. Zhou, Y. Li, S. Chen et al., "Dynamic Agent of an Injectable and Self-Healing Drug-Loaded Hydrogel for Embolization Rherapy," *Colloids and Surfaces B, Biointerfaces* 172 (2018): 601–607.

11. E. Jalalvandi, L. R. Hanton, and S. C. Moratti, "Schiff-Base Based Hydrogels as Degradable Platforms for Hydrophobic Drug Delivery," *European Polymer Journal* 90 (2017): 13–24.

12. X. Zhao, H. Wu, B. Guo, R. Dong, Y. Qiu, and P. X. Ma, "Antibacterial Anti-Oxidant Electroactive Injectable Hydrogel as Aelf-Healing Wound Dressing with Hemostasis and Adhesiveness for Cutaneous Wound Healing," *Biomaterials* 122 (2017): 34–47.

13. L. Han, Y. Zhang, X. Lu, K. Wang, Z. Wang, and H. Zhang, "Polydopamine Nanoparticles Modulating Stimuli-Responsive PNIPAM Hydrogels With Cell/Tissue Adhesiveness," *ACS Applied Materials & Interfaces* 8, no. 42 (2016): 29088–29100.

14. H. H. Chao and D. F. Torchiana, "BioGlue: Albumin/Glutaraldehyde Sealant in Cardiac Surgery," *Journal of Cardiac Surgery* 18, no. 6 (2003): 500–503.

15. W. Fürst and A. Banerjee, "Release of Glutaraldehyde From an Albumin-Glutaraldehyde Tissue Adhesive Causes Significant In Vitro and In Vivo Toxicity," *The Annals of Thoracic Surgery* 79 (2005): 1522–1528.

16. N. Artzi, T. Shazly, C. Crespo, A. B. Ramos, H. K. Chenault, and E. R. Edelman, "Characterization of Star Adhesive Sealants Based on PEG/dextran Hydrogels," *Macromolecular Bioscience* 9, no. 8 (2009): 754–765.

17. J. Ren, H. Yang, Y. Wu, et al., "Dynamic Reversible Adhesives Based on Crosslinking Network via Schiff base and Michael addition," *RSC Advances* 12, no. 24 (2022): 15241–15250.

18. H. A. Hegazy, H. H. Moon, D. H. Lee, et al., "Preparation of Polyaspartamide-Based Adhesive Hydrogels via Schiff Base Reaction with Aldehyde-Functionalized Dextran," *Materials Advances* 4, no. 8 (2023): 1989–1997.

19. G. Yang, Y. Li, S. Zhang, et al., "Double-Cross-Linked Hydrogel With Long-Lasting Underwater Adhesion: Enhancement of Maxillofacial In Situ and Onlay Bone Retention," *ACS Applied Materials & Interfaces* 15, no. 40 (2023): 46639–46654.

20. A. Nishiguchi, Y. Kurihara, and T. Taguchi, "Underwater-Adhesive Microparticle Dressing Composed of Hydrophobically-Modified Alaska Pollock Gelatin for Gastrointestinal Tract Wound Healing," *Acta Biomaterialia* 99 (2019): 387–396.

21. S. Ito, K. Nagasaka, H. Komatsu, D. Palai, A. Nishiguchi, and T. Taguchi, "Improved Hydration Property of Tissue Adhesive/Hemostatic Microparticle Based on Hydrophobically-Modified Alaska Pollock Gelatin," *Biomaterials Advances* 159 (2024): 213834.

22. S. Abbina, S. Vappala, P. Kumar, et al., "Hyperbranched Polyglycerols: Recent Advances in Synthesis, Biocompatibility and Biomedical Applications," *Journal of Materials Chemistry B* 5, no. 47 (2017): 9249–9277.

23. P. Dey, Polyglycerol Based Hydrogels for the Immobilization of Catalytically Active Enzymes and As Scaffolds for Cells, Doctoral Thesis Freie Universität Berlin (2015).

24. M. H. M. Oudshoorn, R. Rissmann, J. A. Bouwstra, and W. E. Hennink, "Synthesis and Characterization of Hyperbranched Polyglycerol Hydrogels," *Biomaterials* 27, no. 32 (2006): 5471–5479.

25. D. Steinhilber, R. Haag, and A. L. Sisson, "Multivalent, Biodegradable Polyglycerol Hydrogels," *Advanced Functional Materials* 2011, 34 (2), 118–122.

26. D. Steinhilber, A. L. Sisson, D. Mangoldt, P. Welker, K. Licha, and R. Haag, "Synthesis, Reductive Cleavage, and Cellular Interaction Studies of Biodegradable, Polyglycerol Nanogels," *Advanced Functional Materials* 20, no. 23 (2010): 4133–4138.

27. B. A. de Campos, N. C. B. Da Silva, L. S. Moda, P. Vidinha, and L. P. Maia-Obi, "pH-Sensitive Degradable Oxalic Acid Crosslinked Hyperbranched Polyglycerol Hydrogel for Controlled Drug Release," *Polymers* 15, no. 7 (2023): 1795.

28. S. Salehpour, C. J. Zuliani, and M. A. Dubé, "Synthesis of Novel Stimuli-Responsive Polyglycerol-Based Hydrogels," *Euro J Lipid Sci & Tech* 114, no. 1 (2012): 92–99.

29. S. Balser, Z. Zhao, M. Zharnikov, and A. Terfort, "Effect of the Crosslinking Agent on the Biorepulsive and Mechanical Properties of Polyglycerol Membranes," *Colloids and surfaces B, Biointerfaces* 225 (2023): 113271.

30. B. Thongrom, P. Tang, S. Arora, and R. Haag, "Polyglycerol-Based Hydrogel as Versatile Support Matrix for 3D Multicellular Tumor Spheroid Formation," *Gels* 12, no. 26 (2023): 938.

31. T. Ooya and J. Lee, "Hydrotropic Hydrogels Prepared From Polyglycerol Dendrimers: Enhanced Solubilization and Release of Paclitaxel," *Gels* 8, no. 10 (2022): 614.

32. P. Dey, S. Hemmati-Sadeghi, and R. Haag, "Hydrolytically Degradable, Dendritic Polyglycerol Sulfate Based Injectable Hydrogels Using Strain Promoted Azide–Alkyne Cycloaddition Reaction," *Polymer Chemistry* 7, no. 2 (2016): 375–383.

33. P. Dey, T. Schneider, L. Chiappisi, M. Gradzielski, G. Schulze-Tanzil, and R. Haag, "Mimicking of Chondrocyte Microenvironment Using In Situ Forming Dendritic Polyglycerol Sulfate-Based Synthetic Polyanionic Hydrogels," *Macromolecular Bioscience* 16, no. 4 (2016): 580–590.

34. K. Karakyriazis, V. Lührs, S. Stößlein, I. Grunwald, and A. Hartwig, "Synthesis and Characterization of a Schiff Base Crosslinked Hydrogel Based on Hyperbranched Polyglycerol," *Mater Adv* 4, no. 7 (2023): 1648–1655.

35. A. Sunder, H. Türk, R. Haag, and H. Frey, "Copolymers of Glycidol and Glycidyl Ethers: Design of Branched Polyether Polyols by Combination of Latent Cyclic AB 2 and ABR Monomers," *Macromolecules* 33, no. 21 (2000): 7682–7692.

36. V. Lührs, S. Stößlein, K. Thiel, I. Grunwald, and A. Hartwig, "An In Vitro Bone-to-Bone Adhesion Test Method Using the Compression Shear Test," *International Journal of Adhesion and Adhesives* 111 (2021): 102977.

37. M. Lallemang, L. Yu, W. Cai, et al., "Multivalent Non-Covalent Interactions Lead to Strongest Polymer Adhesion," *Nanoscale* 14, no. 10 (2022): 3768–3776.

38. S. Wu, Y. Yang, S. Wang, et al., "Dextran and Peptide-Based pH-Sensitive Hydrogel Boosts Healing Process in Multidrug-Resistant Bacteria-Infected Wounds," *Carbohydrate Polymers* 2022 (2021): 118994.

39. M. Muhammad, C. Willems, J. Rodríguez-Fernández, G. Gallego-Ferrer, and T. Groth, "Synthesis and Characterization of Oxidized Polysaccharides for In Situ Forming Hydrogels," *Biomolecules* 10 (2020): 1185.

Supporting Information

Additional supporting information can be found online in the Supporting Information section.

Supporting File: mame70103-sup-0001-SuppMat.pdf.